

Is the proton electromagnetic form factor modified in nuclei?

J. Morgenstern^{1,a} and Z.-E. Meziani²

¹ CEA Saclay DSM/DAPNIA/SPhN, F91191, Gif-sur-Yvette Cedex, France

² Temple University, Philadelphia, PA 19122, USA

Received: 1 November 2002 /

Published online: 15 July 2003 – © Società Italiana di Fisica / Springer-Verlag 2003

Abstract. Guided by the recent experimental confirmation of the validity of the Effective Momentum Approximation (EMA) in quasi-elastic scattering off nuclei, we have re-examined the extraction of the Longitudinal and Transverse Response Functions in medium-weight and heavy nuclei. In the EMA we have performed a Rosenbluth separation of the available world data on ^{40}Ca , ^{48}Ca , ^{56}Fe and ^{208}Pb . We find that the Longitudinal Response Function for these nuclei is “quenched” and that the Coulomb sum is not saturated, at odds with recent claims in the literature.

PACS. 25.30.Fj Inelastic electron scattering to continuum

Quasi-elastic electron scattering off nuclei has permitted to investigate the properties of nucleons in nuclei. As the Coulomb response depends quasi-exclusively on nucleonic degrees of freedom, it was proposed that a Rosenbluth separation of the Coulomb and magnetic responses of a nucleus (R_L and R_T , respectively) could test a model-independent property known as the Coulomb Sum Rule (CSR), $S_L(q)$ [1]:

$$S_L(q) = \frac{1}{Z} \int_{0^+}^{\infty} \frac{R_L(q, \omega)}{\tilde{G}_E^2} d\omega. \quad (1)$$

Here $\tilde{G}_E = (G_E^p + N/Z G_E^n) \zeta$ takes into account the nucleon charge form factor inside the nucleus (which is usually taken to be equal to that of a free nucleon) as well as a relativistic correction (ζ) suggested by de Forest [2]. The lower limit of integration 0^+ excludes the elastic peak. In the limit of large q , $C(q)$, which depends on correlations, is predicted to vanish and consequently $S_L(q)$ to be equal to unity. There is a general agreement in non-relativistic theories, that beyond $|\mathbf{q}| = q \sim 500$ MeV/ c , twice the Fermi momentum, $C_L(q)$ is not bigger than a few % (see review paper [3]).

In the last twenty years a large experimental program has been carried out at Bates [4–12], Saclay [13–17] and SLAC [18–20] aimed at the extraction of R_L and R_T for a variety of nuclei. Unfortunately, in the case of medium-weight and heavy nuclei, conclusions reached by different experiments ranged from a full saturation of the CSR to its violation by 30%. As a result, a spectrum of explanations has emerged ranging from questioning the validity

of the experiments (*i.e.*, experimental backgrounds), inadequate Coulomb corrections (especially for heavy nuclei) to suggesting a picture of a “swollen nucleon” in the nuclear medium due to a partial deconfinement [21–25]. Another approach with the relativistic $\sigma - \omega$ model initiated by Walecka [26,27] has been applied to Nuclear Matter calculations with further improvements including RPA correlations [28], to finite nuclei without RPA correlations [29], to finite nuclei with Relativistic RPA correlations (RRPA) and local density approximations [30–33]. Recently, for Nuclear Matter, the $\sigma - \omega$ model has been extended [34] to take into account the internal nucleon structure using the Quark Meson Coupling (QMC) model of Guichon [35]. In these relativistic models the nucleon form factor is changed in the medium due to vacuum polarization with $N\bar{N}$ pairs.

Up to now the Coulomb corrections for inclusive experiments have been evaluated theoretically by two independent groups, one from Trento University [36,37] and the other from Ohio University [38]. The Trento group found that the Effective Momentum Approximation (EMA) agrees with DWBA with an accuracy better than 1%, while the Ohio group derived significant corrections beyond EMA. All useful quantities and equations are defined in [36,37,39,40]. A detailed discussion of the different theoretical approaches can be found in [37]. Previous extractions of R_L and R_T were performed either without Coulomb corrections in [14,15] or by applying the Trento group calculations [17], or by applying the Ohio group calculations [12,41]. This led to questionable results even when Coulomb corrections from either groups were applied, particularly in the region beyond the quasi-elastic peak known as the “dip region”, since meson exchange

^a e-mail: morgenst@hep.saclay.cea.fr

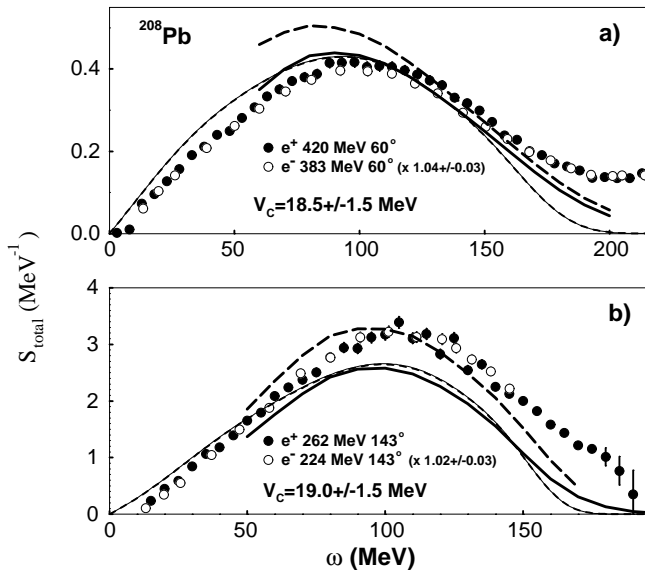


Fig. 1. e^+ (filled circles) and e^- (open circles) total response functions at the same effective incident energies along with the Ohio group calculations (e^+ thick solid lines, e^- thick dashed lines) and the Trento group calculations (e^+ thin solid lines, e^- thin dashed lines).

currents and pion production although significant, were not included in any of the nuclear models used.

A recent comparison of electron and positron quasi-elastic scattering has given an experimental confirmation that EMA can adequately describe the electron and positron over the entire quasi-elastic and dip regions, even for heavy nuclei as we can see in fig. 1.

This experiment has been described in ref. [40]; The positron beam was created by the interaction of a 100 MeV electron beam on a tungsten radiator. The beam emittance was 6 times larger than the emittance of the direct electron beam which results in some uncertainty in the absolute normalization of the measurement. This was overcome by taking in addition electron data, at the same beam intensity (30 nA) and with an emittance downgraded to be comparable to that of the positron beam and controlled with a wire chamber in the beam. These data were taken in kinematics previously measured with a small electron emittance [13,17]. The ratio of the two electron measurements (0.89 and 0.95 at forward and backward angle) allows us to normalize our positron data, which can then be safely compared to the small emittance electron data of [17].

Within EMA the only effect of the Coulomb corrections is to shift the energy of the incident and scattered electron by the average Coulomb potential of the nucleus \widetilde{V}_C :

$$E^i \rightarrow E_{\text{eff}}^i = E^i - \widetilde{V}_C, \quad E^f \rightarrow E_{\text{eff}}^f = E^f - \widetilde{V}_C, \quad (2)$$

$$\omega_{\text{eff}} = E_{\text{eff}}^f - E_{\text{eff}}^i = \omega, \quad (3)$$

$$\overline{\mathbf{q}} = \overline{\mathbf{E}}^f - \overline{\mathbf{E}}^i \rightarrow \overline{\mathbf{q}}_{\text{eff}} = \overline{\mathbf{E}}_{\text{eff}}^f - \overline{\mathbf{E}}_{\text{eff}}^i, \quad (4)$$

and consequently, one can use the Rosenbluth formula where the momentum transfer $|\mathbf{q}|$ is replaced by the effective momentum transfer $|\mathbf{q}_{\text{eff}}|$ as pointed out by Rosenfelder [39].

We present here the results of a re-analysis of the Saclay data only using the Coulomb corrections based on the EMA [42] to extract R_L and R_T and evaluate $S_L(q)$. Our goal was to first determine the change in our previously reported results which either had no Coulomb corrections applied, for ^{40}Ca , ^{48}Ca and ^{56}Fe [14] or for ^{208}Pb [17], had Coulomb corrections applied following a procedure described by Traini *et al.* [36] with the value of the Coulomb potential at the center of the nucleus $V_C(0)$ instead of the average value \widetilde{V}_C .

Next, it was important to test whether including SLAC and Bates data in the EMA analysis would change the results obtained with the Saclay data only.

For that purpose, we present the results obtained with the EMA by combining data on ^{40}Ca , ^{56}Fe , ^{208}Pb from Saclay [14,17], on ^{238}U and ^{40}Ca from Bates [8,12]¹, data on ^{56}Fe at 180° from Bates [6] and data on ^{56}Fe and ^{197}Au from SLAC [18,43]. As ^{208}Pb has been only measured at Saclay, we have combined ^{208}Pb from Saclay with ^{197}Au measured at SLAC and ^{238}U measured at Bates which have close values of Fermi momenta. We have normalized ^{197}Au and ^{238}U cross-sections to ^{208}Pb cross-section, for identical kinematics, using the factor

$$\mathbf{K} = Z[(\epsilon\sigma_{ep}^L + \sigma_{ep}^T) + N(\epsilon\sigma_{en}^L + \sigma_{en}^T)], \quad (5)$$

where ϵ is the virtual-photon polarization and $\sigma_{ep(n)}^{L(T)}$ is the longitudinal (transverse) virtual photon-proton (-neutron) cross-section.

\mathbf{K} is equal to 1.05 for ^{197}Au and 0.88 for ^{238}U .

Figure 2a represents the longitudinal response R_L of ^{56}Fe at $q_{\text{eff}} = 500 \text{ MeV}/c$ obtained with Saclay data (filled circles) and Saclay data combined with SLAC data [43] and Bates data measured at 180° [6]. These data have been compared to non-relativistic microscopic calculations in Nuclear Matter (NM) [44] and Hartree-Fock calculations in ^{56}Fe (HF) [45], taking into account short-range correlations and final-state interactions. These calculations have been performed with free proton form factors and modified proton form factors according to Brown-Rho scaling (BR) [46]. We can see that the agreement of HF with the data is quite good with modified form factors; for NM if the agreement with the data is improved with modified form factor, the calculation gives a too broad response. The same behaviour is observed for ^{208}Pb in fig. 3a.

Figure 2b compares the same data to relativistic calculations using the $\sigma - \omega$ model with RRPA in Nuclear Matter [28] and in ^{56}Fe using a local density approximation [33]. The agreement with the data is better than the non-relativistic HF calculations with free proton form factors, but less good than with modified form factors.

¹ As explained in ref. [42], concerning Bates experiments [8, 12], only data taken with the modified scattering chamber has been taken into account.

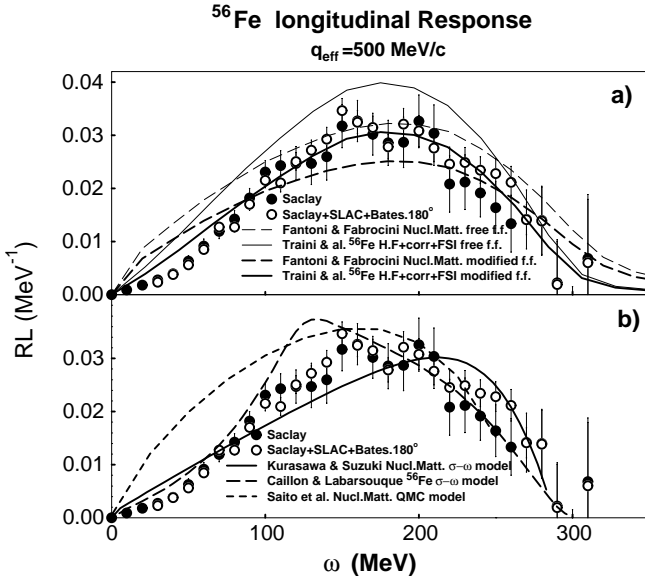


Fig. 2. Longitudinal response function at $q_{\text{eff}}=500\text{MeV}/c$ of ^{56}Fe compared to different theoretical models, non-relativistic (a), relativistic (b).

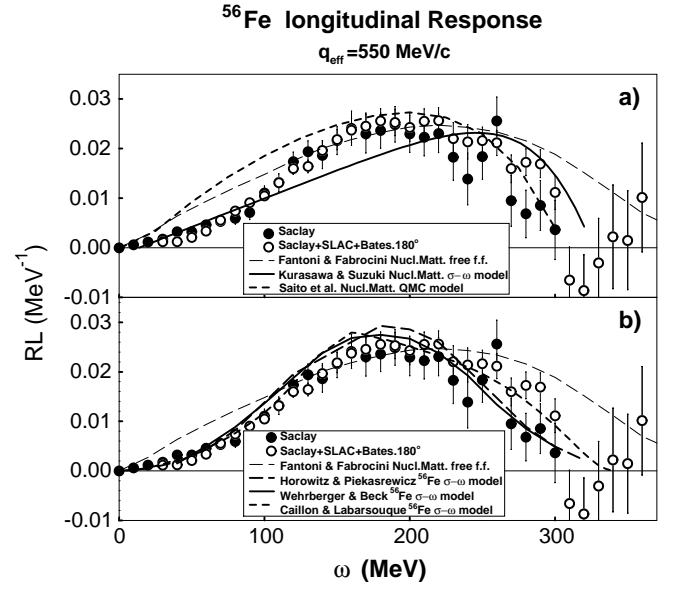


Fig. 4. Longitudinal response function at $q_{\text{eff}}=550\text{MeV}/c$ of ^{56}Fe compared to different theoretical models (see text).

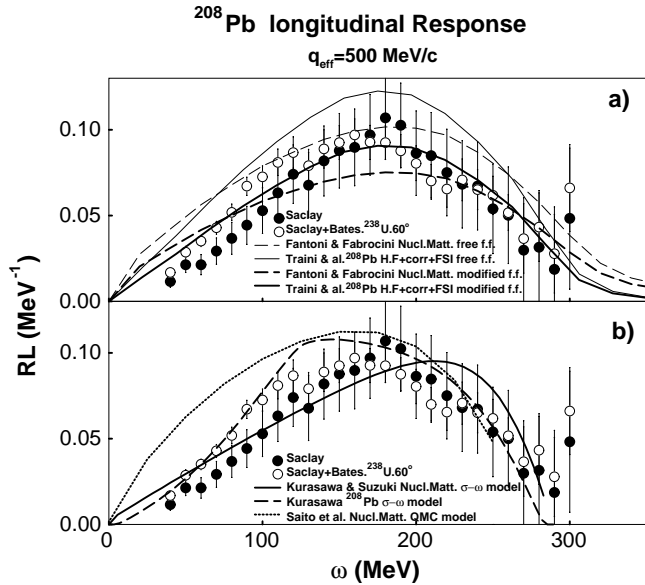


Fig. 3. Longitudinal response function at $q_{\text{eff}}=500\text{MeV}/c$ of ^{208}Pb compared to different theoretical models (see text).

We have shown also the calculation in NM using the QMC model [34], the agreement with the data is less good.

An analog behaviour can be observed for NM relativistic calculations [28,34] in fig. 3b for ^{208}Pb . The agreement is improved with the calculation [28] applied to ^{208}Pb with a local density approximation [47] improves the agreement with the data (fig. 3b dashed line).

Figure 4a shows the comparison of the ^{56}Fe longitudinal response at $q_{\text{eff}} = 550 \text{ MeV}/c$ with the same relativistic calculations in Nuclear Matter as the previous fig-

ures [28,34]. We have represented also the non-relativistic calculation with the free form factor of ref. [44].

Figure 4b shows the comparison of the data with available relativistic calculations in ^{56}Fe at $q_{\text{eff}} = 550 \text{ MeV}/c$ including RPA [30,31,33]; we observe a quite good agreement with the data. We reach the same conclusions as previously.

Finally, we show in fig. 5a the Coulomb Sum Rule (CSR) for ^{40}Ca , ^{48}Ca , ^{56}Fe and ^{208}Pb obtained with the Saclay data only using the EMA analysis. In fig. 5b we have included data from Bates and SLAC-NE3 together with Saclay data to perform Rosenbluth separation. We have used the Simon *et al.* [48] parametrization of the proton charge form factor and the Herberg *et al.* [49] parametrization for the neutron charge form factor. We show also the SLAC-NE9 result at $q = 1140 \text{ MeV}/c$.

Microscopic non-relativistic Nuclear Matter calculation [44] of the *total CSR*, represented by the thick solid line, exhibits only a few percent quenching beyond $q_{\text{eff}} \sim 500 \text{ MeV}/c$.

To compare the experimental results to the theoretical calculations, we have integrated the latter *within the experimental ω domain*.

The long-dashed curve represents the non-relativistic microscopic NM calculation [44]. We find that the experimental CSR evaluated with the correct Coulomb corrections is not saturated, and “quenched” by $\sim 25\text{--}30\%$ in all medium and heavy nuclei, contrary to the analysis by Jourdan [41], represented by the star in fig. 5b, who has applied the Ohio group Coulomb distortions calculation [38].

This quenching corresponds to an increase by $13 \pm 4\%$ of the proton r.m.s. radius for a dipole form factor.

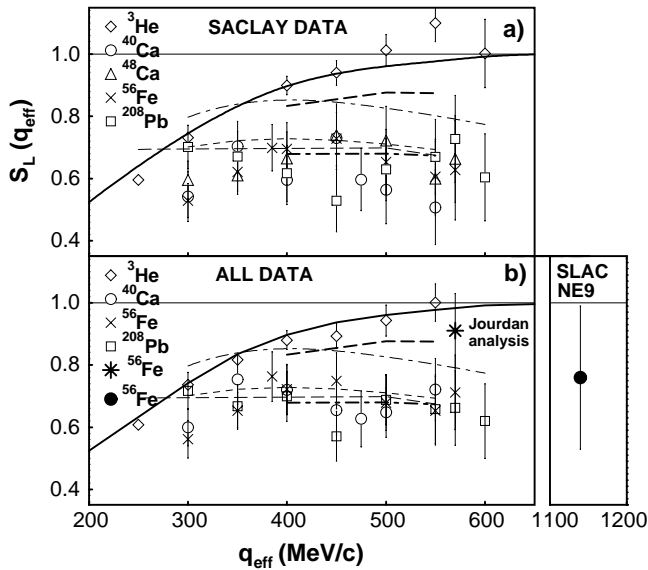


Fig. 5. Experimental CSR obtained with EMA compared to different theoretical models (see text).

The thick dot-dashed curve represents the former calculations with modified form factor according to Brown-Rho scaling which agree fairly well with the data.

Non-relativistic Hartree-Fock calculations in ^{208}Pb at $q_{\text{eff}} = 400$ and 500 MeV/c, including short-range correlations and final-state interactions [45] give very close values to the NM calculations and cannot be distinguished in the figure².

The thin long-dashed and the thin dashed curves represent, respectively, the relativistic calculations in NM and in ^{56}Fe within the $\sigma - \omega$ model with RPA [28,33]. The thin dotted curve represent the relativistic calculation in NM [34] within the QMC model [35]. The comparison of the experimental CSR with the theoretical calculations are the same as in the discussion of figs. 3, 4, 5.

In conclusion, the observed quenching of the CSR gives a serious indication for a change of the nucleon form factor with the nuclear density. No appreciable quenching is seen in ^3He , as shown in fig. 5.

The present experiments will be extended until $q_{\text{eff}} = 1$ GeV/c in an approved experiment at TJNAF [50].

BR scaling and $\sigma - \omega$ model calculations predict a very small change of the transverse response because the nucleon free mass is replaced by the nucleon effective mass in the denominator of the magnetic operator. This explains the observed y scaling in the SLAC experiments at high momentum transfers [43]. In these experiments where no longitudinal-transverse separation have been performed, the longitudinal component represents less than 20% of the total cross-section; consequently a 30% quenching of

² In a previous paper [42] we have found $\sim 5\%$ difference because we had taken the Simon *et al.* [48] proton form factor to evaluate the HF CSR instead of the dipole one used by the authors [45] to calculate the longitudinal response.

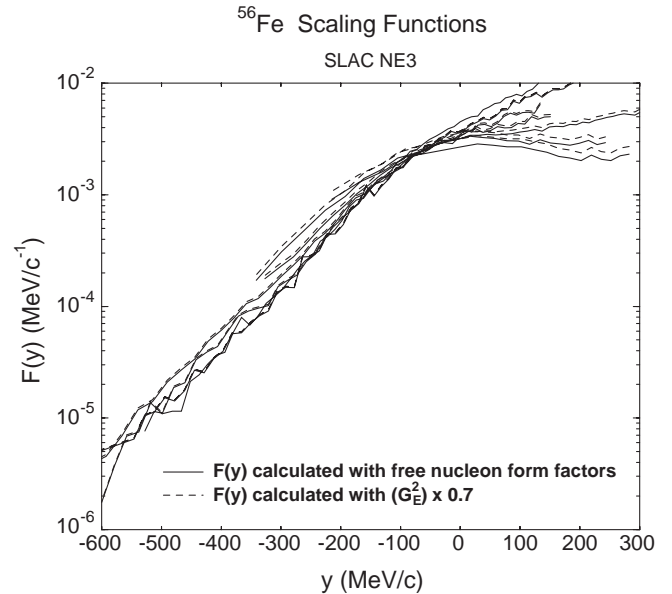


Fig. 6. ^{56}Fe scaling function evaluated with free and medium modified proton Coulomb response (see text).

the Longitudinal Response results in a 6% quenching of the unseparated response.

In fig. 6, we have shown the scaling analysis of the SLAC experiment [43] (solid curves) and the same analysis with a 30% quenching of the longitudinal proton response (dashed curve). The shift between the solid and the dashed curves is much smaller than the dispersion of the scaling curves; consequently the quenching observed in the longitudinal response is not in contradiction with the y scaling observed at high momentum transfers [43].

References

1. K.W. McVoy, L. Van Hove, Phys. Rev. **125**, 1034 (1962).
2. T. de Forest jr., Nucl. Phys. A **414**, 347 (1984).
3. G. Orlandini, M. Traini, Rep. Prog. Phys. **54**, 257 (1991).
4. R. Altemus *et al.*, Phys. Rev. Lett. **44**, 965 (1980).
5. M. Deady *et al.*, Phys. Rev. C **28**, 8 (1983) 631.
6. A. Hotta *et al.*, Phys. Rev. C **30**, 87 (1984).
7. M. Deady *et al.*, Phys. Rev. C **33**, 1897 (1986).
8. C.C. Blatchley *et al.*, Phys. Rev. C **34**, 1243 (1986).
9. S.A. Dytman *et al.*, Phys. Rev. C **38**, 800 (1988).
10. K. Dow *et al.*, Phys. Rev. Lett. **61**, 1706 (1988); K. Dow, private communication.
11. T.C. Yates *et al.*, Phys. Lett. B **312**, 382 (1993).
12. C. Williamson *et al.*, Phys. Rev. C **56**, 3152 (1997).
13. P. Barreau *et al.*, Nucl. Phys. A **402**, 515 (1983).
14. Z.-E. Meziani *et al.*, Phys. Rev. Lett. **52**, 2130 (1984).
15. Z.-E. Meziani *et al.*, Phys. Rev. Lett. **54**, 1233 (1985).
16. C. Marchand *et al.*, Phys. Lett. B **153**, 29 (1985).
17. A. Zghiche *et al.*, Nucl. Phys. A **572**, 513 (1994).
18. D.T. Baran *et al.*, Phys. Rev. Lett. **61**, 400 (1988).
19. J.P. Chen *et al.*, Phys. Rev. Lett. **66**, 1283 (1991).
20. Z.-E. Meziani *et al.*, Phys. Rev. Lett. **69**, 41 (1992).
21. J.V. Noble, Phys. Rev. Lett. **46**, 412 (1981).

22. L.S. Celenza *et al.*, Phys. Rev. Lett. **53**, 891 (1984).
23. P.J. Mulders, Nucl. Phys. A **459**, 525 (1986).
24. M. Ericson, M. Rosa-Clot, Z. Phys. A **324**, 373 (1986).
25. G.E. Brown, M. Rho, Phys. Lett. B **222**, 324 (1989).
26. J.D. Walecka, Ann. Phys. (N.Y.) **83**, 491 (1974).
27. B.D. Serot, J.D. Walecka, Adv. Nucl. Phys. **16**, 1 (1986).
28. H. Kurasawa, T. Suzuki, Phys. Lett. B. **208**, 160 (1988); **211**, 500 (1988) (E); Prog. Theor. Phys. **84**, 1030 (1990).
29. G. Do Dang, Nguyen Van Giai, Phys. Rev. C **30**, 731 (1984).
30. C.J. Horowitz, J. Piekarewicz, Phys. Rev. Lett. **62**, 391 (1989); Nucl. Phys. A **511**, 461 (1990).
31. K. Wehrberger, F. Beck, Nucl. Phys. A **491**, 587 (1989).
32. R. Brockmann, H. Toki, Phys. Rev. Lett. **68**, 3408 (1992).
33. J.C. Caillon, J. Labarsouque, Nucl. Phys. A **595**, 189 (1995).
34. K. Saito, K. Tsushima, A.W. Thomas, Phys. Lett. B **465**, 27 (1999).
35. P.A.M. Guichon, Phys. Lett. B **200**, 235 (1988).
36. M. Traini, S. Turck-Chièze, A. Zghiche, Phys. Rev. C **38**, 2799 (1988); M. Traini, M. Covi, Nuovo Cimento A **108**, 723 (1995); M. Traini, Nuovo Cimento A **108**, 1259 (1995).
37. M. Traini, Nucl. Phys. A **694**, 325 (2001).
38. D. Onley, Y. Yin, L.E. Wright, Phys. Rev. C **45**, 1333 (1992); K.S. Kim, L.E. Wright, Y. Yin, D.W. Kosik, Phys. Rev. C **54**, 2515 (1996); K.S. Kim, L.E. Wright, D.A. Resler, Phys. Rev. C **64**, 044607 (2001).
39. R. Rosenfelder, Ann. Phys. (N.Y.) **128**, 188 (1980).
40. P. Gueye *et al.*, Phys. Rev. C **60**, 044308 (1999).
41. J. Jourdan, Phys. Lett. B **353**, 189 (1995); Nucl. Phys. A **603**, 117 (1996).
42. J. Morgenstern, Z.-E. Meziani, Phys. Lett. B **515**, 269 (2001).
43. D. Day *et al.*, Phys. Rev. C **48**, 1849 (1993).
44. A. Fabrocini, S. Fantoni, Nucl. Phys. A **503**, 375 (1989).
45. M. Traini, G. Orlandini, W. Leidemann, Phys. Rev. C **48**, 172 (1993).
46. M. Soyeur, G.E. Brown, M. Rho, Nucl. Phys. A **556**, 355 (1993).
47. H. Kurasawa, private communication (2002).
48. G.G. Simon *et al.*, Nucl. Phys. A **333**, 381 (1980).
49. C. Herberg *et al.*, Eur. Phys. J. A **5**, 131 (1999).
50. JLab experiment E01-016; Spokespeople: Seonho Choi, J. P. Chen, Z.-E. Meziani.